



# High light quantity suppresses locomotion in symbiotic *Aiptasia*

Nils F. Strumpen<sup>1</sup> · Nils Rådecker<sup>1,2</sup> · Claudia Pogoreutz<sup>1,2</sup> · Anders Meibom<sup>2,3</sup> · Christian R. Voelstra<sup>1</sup>

Received: 10 January 2022 / Accepted: 30 April 2022  
© The Author(s) 2022

## Abstract

Many cnidarians engage in endosymbioses with microalgae of the family Symbiodiniaceae. In this association, the fitness of the cnidarian host is closely linked to the photosynthetic performance of its microalgal symbionts. Phototaxis may enable semi-sessile cnidarians to optimize the light regime for their microalgal symbionts. Indeed, phototaxis and phototropism have been reported in the photosymbiotic sea anemone *Aiptasia*. However, the influence of light quantity on the locomotive behavior of *Aiptasia* remains unknown. Here we show that light quantity and the presence of microalgal symbionts modulate the phototactic behavior in *Aiptasia*. Although photosymbiotic *Aiptasia* were observed to move in seemingly random directions along an experimental light gradient, their probability of locomotion depended on light quantity. As photosymbiotic animals were highly mobile in low light but almost immobile at high light quantities, photosymbiotic *Aiptasia* at low light quantities exhibited an effective net movement towards light levels sufficient for positive net photosynthesis. In contrast, aposymbiotic *Aiptasia* exhibited greater mobility than their photosymbiotic counterparts, regardless of light quantity. Our results suggest that photosynthetic activity of the microalgal symbionts suppresses locomotion in *Aiptasia*, likely by supporting a positive energy balance in the host. We propose that motile photosymbiotic organisms can develop phototactic behavior as a consequence of starvation linked to symbiotic nutrient cycling.

**Keywords** Cnidarian-algal symbiosis · *Exaiptasia diaphana* · Movement · Phototaxis · Symbiodiniaceae

## 1 Introduction

Sessile Cnidaria, particularly scleractinian corals, form the structural and ecological foundation of coral reef ecosystems. Their ecological success in the oligotrophic tropical ocean is related to their symbiosis with intracellular microalgae (Symbiodiniaceae, Dinoflagellata; LaJeunesse et al. 2018), which provide a major source of energy for their hosts through photosynthetic activity (Sheppard et al. 2017). The metabolic coupling between phototrophic symbionts and their heterotrophic host provides the framework

for efficient exchange and recycling of energy and nutrients between both partners (Muscatine and Porter 1977; Furla et al. 2000; Papina et al. 2003; Kopp et al. 2015; Rådecker et al. 2015, 2021). The functioning of the symbiosis therefore depends on the photosynthetic activity of the microalgae and consequently light availability. The cnidarian-algal symbiosis occurs across a broad range of environmental light regimes (Kleypas et al. 1999). These differences in light availability imposed by latitude, water depth, seasonality, turbidity, cloud cover, and tides imply that the ecological success of the cnidarian-algal symbiosis stems from its ability to make effective use of the available photosynthetically active radiation (PAR, light of wavelength in the range of 400–700 nm), while at the same time avoiding photodamage (Baker and Weber 1975; Anthony et al. 2004; Grigg 2005; Muir et al. 2015; Ziegler et al. 2015b).

Photosymbiotic cnidarians may adapt or acclimate to different light regimes in multiple ways. The endosymbiotic microalgae possess an arsenal of photophysiological responses that facilitate short- and medium-term light acclimation, including adjustments of the photosynthetic electron transport, light harvesting complexes, and photopigments (as

✉ Nils F. Strumpen  
nils-fabian.strumpen@uni-konstanz.de

<sup>1</sup> Department of Biology, University of Konstanz, Konstanz, Germany

<sup>2</sup> Laboratory for Biological Geochemistry, School of Architecture, Civil and Environmental Engineering, École Polytechnique Fédérale de Lausanne, Lausanne, Switzerland

<sup>3</sup> Center for Advanced Surface Analysis, Institute of Earth Sciences, University of Lausanne, Lausanne, Switzerland

reviewed by Eberhard et al. 2008). The cnidarian host has the ability to modulate the amount of light penetrating the tissues through the production of fluorescent pigments either for photoprotection (Salih et al. 2000) or wavelength transformation to enhance microalgal photosynthesis depending on the light regime (Smith et al. 2017). In the case of corals, their skeletal structure can also modulate incoming irradiance through its light scattering properties (Kaniewska et al. 2011; Kahng et al. 2012). Furthermore, cnidarian hosts may compensate for reduced photosynthate translocation at lower light levels through a high degree of trophic plasticity, i.e., they can increase the level of heterotrophic feeding in low light environments (Muscatine et al. 1989; Anthony and Fabricius 2000; Ziegler et al. 2014). Dynamic changes in microalgal symbiont types or densities within the host tissue may further aid acclimation to different light regimes and optimize symbiotic nutrient cycling (Titlyanov et al. 2001). Finally, different microalgal symbiont species might also be adapted to different light regimes (Baker and Weber 1975; Cooper et al. 2011; Wall et al. 2020). As algal symbiont communities can differ among cnidarian host species (Iglesias-Prieto et al. 2004), among colonies of the same species (Frade et al. 2008), or even within a single colony (Rowan and Knowlton 1995), changes in microalgal community composition also represent a potential mechanism of light acclimation (Ziegler et al. 2015a, b).

Compared to adjustments in holobiont physiology and composition, a more direct approach to light acclimation is phototaxis, the directed locomotion in response to a light stimulus. Phototaxis is observed in many mobile organisms but is especially relevant for phototrophic organisms. This includes cyanobacteria, eukaryotic microalgae, multicellular algae (as reviewed by Jekely 2009), and organisms secondarily phototrophic through symbiosis or kleptoplasty, e.g., the ciliate *Paramecium bursaria* (Iwatsuki and Naitoh 1981), the acoelomorph worm *Symsagittifera roscoffensis* (Serôdio et al. 2011), or sacoglossan sea slugs (Miyamoto et al. 2015). Phototaxis may allow the phototrophic organism to move towards a specific light regime that allows for optimal photosynthetic activity or to move away from detrimental high light environments to avoid photodamage.

Although larvae of scleractinian corals are mobile and exhibit phototactic behavior (Mundy and Babcock 1998), their colonial adult counterparts are largely immobile, apart from passive transportation, e.g., after fragmentation (Highsmith 1982), and some mobile exceptions like the Fungiidae (Yamashiro and Nishira 1995). However, such immobility is not the case for other photosymbiotic cnidarians with a semi-sessile lifestyle, notably sea anemones (Actiniaria). Actiniaria are closely related to scleractinian corals and commonly associate with the same or similar microalgal symbionts but retain a degree of mobility despite their sessile lifestyle. Actiniaria are mobile either by movement with

the help of their pedal discs or by floating detached as part of their life history, for dispersing, seeking out prey, avoiding predators, or avoiding being buried by sediment (as reviewed by Riemann-Zürneck 1998). Actiniarian motility has also been shown to include phototactic behavior with a potential role in photoacclimation (Pearse 1974; Riemann-Zürneck 1998; Foo et al. 2019).

Despite the putative importance of mobile behavior, the underlying drivers of locomotion and phototaxis in photosymbiotic Actiniaria (Dungan et al. 2020) remain poorly understood. It has been reported that phototactic behavior is modified by light quality and the presence of algal symbionts in the sea anemones *Anthopleura elegantissima* and *Exaiptasia diaphana*, implying that phototaxis in these Actiniaria is an exclusive property of photosymbiotic individuals (Pearse 1974; Foo et al. 2019). It has also been suggested that locomotion in Actiniaria (e.g., Aiptasia) may be induced by heterotrophic starvation (Bedgood et al. 2020). However, the role of nutrition in the phototactic behavior of *A. elegantissima* remains to be determined.

Here, we investigate the effects of light quantity on locomotion in the coral model Aiptasia, sensu *E. diaphana* (Dungan et al. 2020). These anemones naturally occur in tropical and subtropical shallow marine habitats such as shaded mangrove roots (Cook et al. 1988). The extreme tidal, diurnal, and seasonal environmental variability of these habitats coupled with the absence of fluorescent proteins such as GFP in the genome of Aiptasia (Baumgarten et al. 2015), suggest that locomotion may be an important trait in this anemone to optimize light conditions for their algal symbionts. While most photosymbiotic Cnidaria depend on their algal symbionts for survival, Aiptasia can be maintained in an aposymbiotic (algae-free) state if sufficient food is available (Weis et al. 2008). Harnessing these advantages, in this study we compare the movement of photosymbiotic and aposymbiotic Aiptasia in an experimentally controlled light gradient to investigate how light quantity affects phototaxis and associated net photosynthesis. This approach allowed us to link behavioral differences to the photophysiology of the photosymbiotic holobiont.

## 2 Materials & methods

### 2.1 Aiptasia strain

Photosymbiotic and aposymbiotic anemones of the Aiptasia strain CC7 (Sunagawa et al. 2009) were used for all experiments. Photosymbiotic CC7 harbored their native algal symbiont community dominated by strain SSA01 of *Symbiodinium linucheae* (Bieri et al. 2016). Aposymbiotic CC7 animals were generated by removal of algal symbionts using the cold shock bleaching protocol as outlined

previously (Pringle Lab 2018). Complete removal of symbionts was accomplished by an 8 week-long treatment in artificial seawater (ASW, see 2.2.) containing 50  $\mu\text{M}$  DCMU under constant 50  $\mu\text{E m}^{-2} \text{s}^{-1}$  illumination. Absence of algal symbionts in aposymbiotic animals was confirmed by fluorescence stereomicroscopy.

## 2.2 *Aiptasia* rearing

All anemones were maintained at 25 °C in transparent 2 L plastic boxes filled with artificial seawater (ASW; salinity 34 – 36 ‰) prepared from Pro-Reef sea salt (Tropic Marin AG, Hünenberg, Switzerland).

Photosymbiotic *Aiptasia* were maintained at a 12:12 day:night light cycle for over 3 months before the start of the experiment with 60  $\mu\text{E m}^{-2} \text{s}^{-1}$  on PSI LED cultivation shelves (Photon Systems Instruments, Drásov, Czech Republic). The light sources were arranged in LED strips parallel to the long edge of the shelf. Spacing of LEDs decreased towards the edges to ensure a homogenous light field on the shelves. The light quantity was chosen based on preliminary experiments that demonstrated optimal growth of *Aiptasia* between 50 and 70  $\mu\text{E m}^{-2} \text{s}^{-1}$ , while avoiding excessive photodamage. Aposymbiotic animals were maintained in the dark for 3 months before the start of the experiment. All animals were fed weekly with freshly hatched *Artemia salina* nauplii. One day after feeding, the boxes were thoroughly cleaned with cotton swabs and the ASW was fully exchanged.

## 2.3 Locomotion along a light gradient

To record the locomotive response of *Aiptasia* to different light quantities, the movement of individuals was tracked along a defined light gradient using a custom-built experimental setup (Fig. 1). The interior of the black PVC boxes measured 60 cm on the long side and 39.3 cm on the short side and 3 cm in height. Each box was subdivided into 12 individual racetracks (i.e., compartments with the following dimensions: 60 cm long and 3 cm wide) by removable, 3 mm thick PVC separators. Each box was filled with 5 L ASW (salinity 34 – 36 ‰; height of water column ~2.5 cm). Limited water exchange between the racetracks within a PVC box was therefore possible, however, *Aiptasia* were unable to physically cross between them. The boxes were covered with transparent acrylic glass (PMMA) lids. The lids were laminated with a printed-on black-transparent gradient foil (transparent PVC foil print, Bannerkönig GmbH, Gelsenkirchen, Germany).

The boxes were placed on PSI LED cultivation shelves. Light quantity and distance from the light source were adjusted so that the resulting PAR gradient in the PVC boxes ranged from 2  $\mu\text{E m}^{-2} \text{s}^{-1}$  to 101  $\mu\text{E m}^{-2} \text{s}^{-1}$  with a

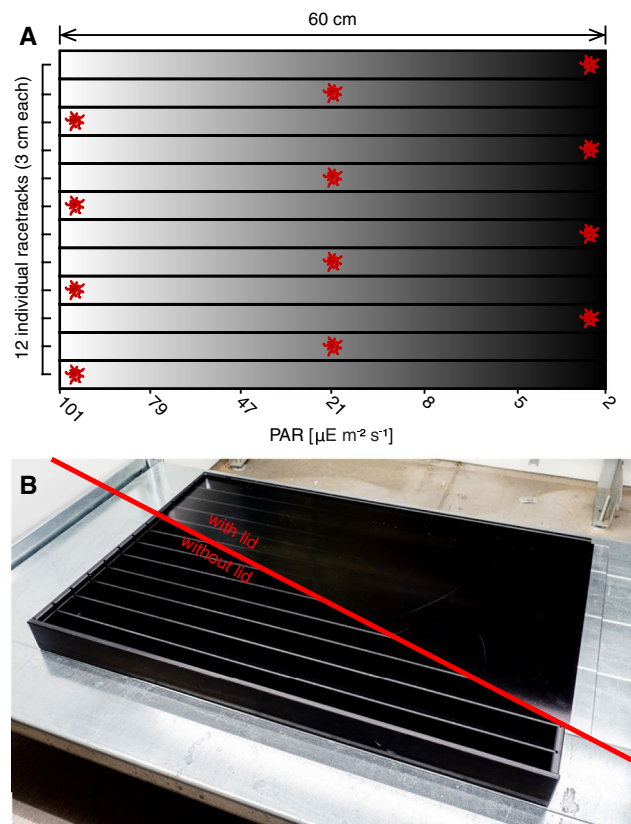


**Fig. 1** Experimental locomotion light gradient setup. (A) Schematic illustration of the setup used to track the movement of individual *Aiptasia* along a defined gradient of photosynthetically active radiation (PAR). *Aiptasia* (red) refer to individual anemones placed in one of three possible starting positions in the experimental setup. Each setup consisted of a shallow PVC box subdivided into 12 individual racetracks. The boxes were covered with an acrylic glass lid with a transparency gradient to achieve the light gradient. (B) Photograph of the setup without (bottom-left) and with (top-right) lid installed

logistic increase from low to high light quantity. PAR levels were quantified with a MQ-500 Quantum Meter (Apogee Instruments, Inc., Logan, USA). The light was set to a 24:0 day:night cycle (constant light) to ensure temporal consistency of the light gradient and the temperature was maintained at 25 °C.

A total of six 42-day experimental runs was performed in the described boxes, i.e., three runs with photosymbiotic ( $n = 36$  animals) and three runs with aposymbiotic ( $n = 36$  animals) *Aiptasia*. For each experimental run, *Aiptasia* were placed at one of three different starting positions: four animals each at low ( $\sim 2 \mu\text{E m}^{-2} \text{s}^{-1}$ ), intermediate ( $\sim 21 \mu\text{E m}^{-2} \text{s}^{-1}$ ), and high ( $\sim 101 \mu\text{E m}^{-2} \text{s}^{-1}$ ) light quantities (Fig. 1A; 4 animals per starting position for each of the three runs = 12 animals per starting position and symbiotic state). At the beginning of each run, individual *Aiptasia* last fed 7 days prior to the experiment were placed in each of the racetracks. *Aiptasia* were taken directly from their rearing

conditions without further acclimation. The photosymbiotic and aposymbiotic individuals used for the experiment had a pedal disk diameter of 3–5 mm and 2–3 mm, respectively. The position of each *Aiptasia* in the one-dimensional orientation of the gradient was recorded daily for 42 days with an accuracy of about  $\pm 4$  mm by manual placement of a ruler next to the racetrack and without moving the box. The position of an *Aiptasia* was defined by the position of the center of the pedal disc regardless of the orientation or attachment of the animal. ASW was exchanged every week. During the process of water exchange, the compartment separators were removed. Detached *Aiptasia* were carefully collected and reinserted at their last known position after the ASW exchange.

## 2.4 Net photosynthesis along a light gradient

Net photosynthetic performance of *Aiptasia* holobionts was measured across the previously defined light gradient. Oxygen ( $O_2$ ) fluxes were recorded at distinct light quantities spanning the entire range of the light gradient, namely 0, 17, 33, 50, 67, 83, and 100  $\mu E m^{-2} s^{-1}$ . To measure the photosynthetic response, photosymbiotic *Aiptasia* last fed 6–7 days prior to the experiment were placed individually in black PVC boxes measuring 10  $\times$  10 cm on the inside filled with 200 mL ASW and covered with a transparent PMMA lid. Anemones were incubated for 24 h at the respective PAR level on PSI LED cultivation shelves to acclimatize to the respective conditions.

After the 24 h incubation, anemones were transferred underwater into 12.3 mL borosilicate vials in a water bath filled with ASW; anemones were allowed to attach to the vial for 2 h in the dark. After approximately 2 h, anemones were fully attached at or near the bottom of their respective vial. A 6 mm magnetic stirrer was inserted into each vial, and vials were turned upside down and screwed to their lids attached to the bottom of the water bath under total air exclusion. The water bath was placed on a magnetic multi stirrer and set to 240 rpm at the respective light quantity. This ensured that dissolved  $O_2$  gradients or layering were avoided in the vials over the course of the experiment. Likewise, the ASW in the water bath was constantly mixed to ensure a constant temperature of 25 °C throughout the experiment.

$O_2$  concentrations were measured using FSO2-4 Oxygen meters (PyroScience GmbH, Aachen, Germany). OXSP5  $O_2$  sensor spots glued to the inside of the vials connected with 2 m SPFIB-BARE-CL2 cables, a TSUB21 Temperature sensor in the water bath, and the internal pressure sensor of the FSO2-4 were used to collect all data necessary for the determination of  $O_2$  concentrations. The raw  $O_2$  concentration was computed and recorded using the software Pyro Oxygen Logger.

The  $O_2$  concentrations were recorded at the respective light quantity every 5 s for 2–5 h until a steady linear change of  $O_2$  concentration had been observed for at least 30 min. For each light quantity, 6 *Aiptasia* and 2 ASW controls were recorded.

In order to normalize the net  $O_2$  flux measurements, algal symbiont cells were isolated and quantified from each *Aiptasia*. *Aiptasia* were transferred into pre-weighed 2 mL round-bottom microreaction tubes. Care was taken not to transfer any seawater, and 1X phosphate buffered saline (PBS; AppliChem GmbH, Darmstadt, Germany) was added to the animal to a final weight of 0.5 g. Then, animals were homogenized for 30 s with a PT 1200 E disperser (Kinematica AG, Malters, Switzerland) at maximum speed. Afterwards, the homogenate was centrifuged at 3000  $\times$  g at 21 °C for 3 min. The supernatant was discarded, and the pellet was resuspended by vigorous vortexing in 1X PBS (added up to a final weight of 0.5 g). Microalgal symbiont cell counts for each anemone were then determined using a Countess II FL Automated Cell Counter (Thermo Fisher Scientific Inc., Waltham, USA) with a Cy5 light cube. Microalgal symbiont cells were identified by their size and their chlorophyll fluorescence in the Cy5 channel.

## 2.5 Data analysis

All data were analyzed in R 4.0.3 (R Core Team 2020). The normality of residuals of all data from the locomotion experiment was tested with Shapiro–Wilk tests and homoscedasticity was tested with Levene’s tests.

All data from aposymbiotic and photosymbiotic *Aiptasia* were analyzed separately. For all analyses, data were considered as independent since all animals derived from the same clonal population were reared under identical conditions, and were of similar sizes. In cases where the residuals of a model were normally distributed and homoscedasticity was not violated (this was the case for the start–end position difference for aposymbiotic animals), a one-way ANOVA based on starting position was performed followed by a Tukey’s HSD post-hoc test for pairwise comparisons. Where model residuals were not normally distributed or homoscedasticity was violated, a non-parametric Kruskal–Wallis test and a pairwise Wilcoxon–Mann–Whitney test with Bonferroni correction on non-transformed data were used for the analysis of variance and pairwise comparison, respectively. This was the case for all data except start–end-position difference for aposymbiotic animals. When comparing end and starting position, the position at day 1 instead of the assumed starting position day 0 was used. Only data points of subsequent days were considered and day 0 was excluded as well when addressing daily movements. A model for the probability of locomotive movement per any given position along the gradient was developed. This was done by assigning all

daily position differences  $\geq 0.5$  cm d<sup>-1</sup> the value 1 (movement) and all other data points the value 0 (no movement). A binomial generalized linear model with a logit link function to the predictor variable, position along the gradient, was fitted to these data.

To compare the overall probabilities of movements between the two symbiotic states, the same binomial generalized linear model approach was used and tested with an analysis of deviance  $\chi^2$  test. Additionally, overall mean absolute, absolute daily, and directional daily movement between the two symbiotic states were tested with Wilcoxon–Mann–Whitney tests with continuity correction.

The package LoLinR (Olito et al. 2017) was used to reproducibly obtain O<sub>2</sub> flux rates from a linear subset of the recorded change in O<sub>2</sub> concentrations. Meaningful regression could not be applied to 2 replicates (both at 83  $\mu\text{E m}^{-2} \text{s}^{-1}$ ) which were subsequently removed from further analysis. The mean O<sub>2</sub> flux rates of the ASW controls (to account for potential background O<sub>2</sub> fluxes) were subtracted from each rate measurement to obtain the respective net O<sub>2</sub> flux rates. The net O<sub>2</sub> flux rates were normalized by dividing by the respective algal symbiont cell count of the animal. A second-degree polynomial regression was fitted to O<sub>2</sub> flux rates dependent on PAR level to assess the effect of light quantity on the photosynthetic response of *Aiptasia*.

## 3 Results

### 3.1 Locomotion along a light gradient

#### 3.1.1 Photosymbiotic *Aiptasia*

Photosymbiotic *Aiptasia* exhibited a mean absolute movement along the gradient (end position – starting position) of  $6.3 \pm 1.5$  cm (mean  $\pm$  standard error) over the course of the experiment and a mean absolute daily movement of  $0.27 \pm 0.04$  cm d<sup>-1</sup>. The movement appeared random, i.e., not predictable regarding its direction along the light gradient, with a mean daily directional movement of only  $0.09 \pm 0.04$  cm d<sup>-1</sup> (towards the light).

However, the pattern of movement was strongly dependent on the position of the animals in the light gradient (Fig. 2 A, D, E). When starting at the dark end of the light gradient (0 cm,  $\sim 2 \mu\text{E m}^{-2} \text{s}^{-1}$ ), animals moved in a chaotic manner, but their mean position shifted towards greater PAR levels over the course of the experiment. At the end of the experiment, their mean position was at  $14.9 \pm 2.8$  cm ( $\sim 6 \mu\text{E m}^{-2} \text{s}^{-1}$ ). The animals starting at the intermediate position (30 cm,  $\sim 21 \mu\text{E m}^{-2} \text{s}^{-1}$ ) and the bright end (60 cm,  $\sim 101 \mu\text{E m}^{-2} \text{s}^{-1}$ ) did rarely move and their mean positions were stable over the course of the experiment. Their end positions

were  $31.1 \pm 1.0$  cm ( $\sim 24 \mu\text{E m}^{-2} \text{s}^{-1}$ ) and  $59.1 \pm 0.6$  cm ( $\sim 100 \mu\text{E m}^{-2} \text{s}^{-1}$ ), respectively.

Therefore, the mean absolute distance photosymbiotic animals moved along the gradient (Fig. 2D) was significantly affected by their starting position (Kruskal–Wallis test,  $\chi^2 = 16.2$ , p-value < 0.001). Animals starting at the dark end of the light gradient showed significantly greater absolute movement compared to animals starting at the intermediate position and the bright end of the light gradient (pairwise Wilcoxon–Mann–Whitney test, p-value = 0.018 and p-value = 0.003, respectively). Likewise, the mean absolute distance moved was significantly greater in animals starting at the intermediate position than in animals starting at the bright light end of the light gradient (pairwise Wilcoxon–Mann–Whitney test, p-value = 0.025).

The mean absolute daily movement of the animals, i.e., the daily movement in any direction, (Fig. 2E) was also significantly affected by their starting position (Kruskal–Wallis test,  $\chi^2 = 132.04$ , p-value < 0.001). The mean absolute daily movement observed was significantly different between any two starting positions (pairwise Wilcoxon–Mann–Whitney test, all p-values < 0.01).

Photosymbiotic animals exhibited an overall low incidence of movement (defined as movement  $\geq 0.5$  cm d<sup>-1</sup>), which occurred at only 9.2% of the recorded daily intervals. A greater probability of movement was observed at positions with low photosynthetically active radiation (PAR) (Fig. 2F), and a significantly lower probability of locomotion was observed with increasing PAR levels (McFadden  $R^2 = 0.175$ ;  $\chi^2 = 94.09$ , p-value < 0.001). The probability of movement when plotted followed an exponential distribution with movement probability declining with increasing PAR levels (from 30.3% at  $2 \mu\text{E m}^{-2} \text{s}^{-1}$  to 0.8% at  $101 \mu\text{E m}^{-2} \text{s}^{-1}$ ).

#### 3.1.2 Aposymbiotic *Aiptasia*

Aposymbiotic *Aiptasia* exhibited a significantly greater mean absolute distance moved along the gradient ( $23.9 \pm 3.2$  cm; Wilcoxon–Mann–Whitney test,  $W = 251.5$ , p-value < 0.001) over the course of the experiment as well as a significantly greater mean absolute daily movement ( $3.32 \pm 0.23$  cm d<sup>-1</sup>; Wilcoxon–Mann–Whitney test,  $W = 197,684$ , p-value < 0.001) in comparison to their photosymbiotic counterparts. The directionality of the movement did not differ significantly from photosymbiotic animals ( $0.03 \pm 0.26$  cm d<sup>-1</sup> (towards the light); Wilcoxon–Mann–Whitney test,  $W = 378,935$ , p-value = 0.369).

The random movement of anemones along the light gradient was independent of their starting position (Fig. 3A, D, E). The mean position of all three groups assessed (starting at low light (0 cm and  $\sim 2 \mu\text{E m}^{-2} \text{s}^{-1}$ ), intermediate light (30 cm and  $\sim 21 \mu\text{E m}^{-2} \text{s}^{-1}$ ), and high light (60 cm

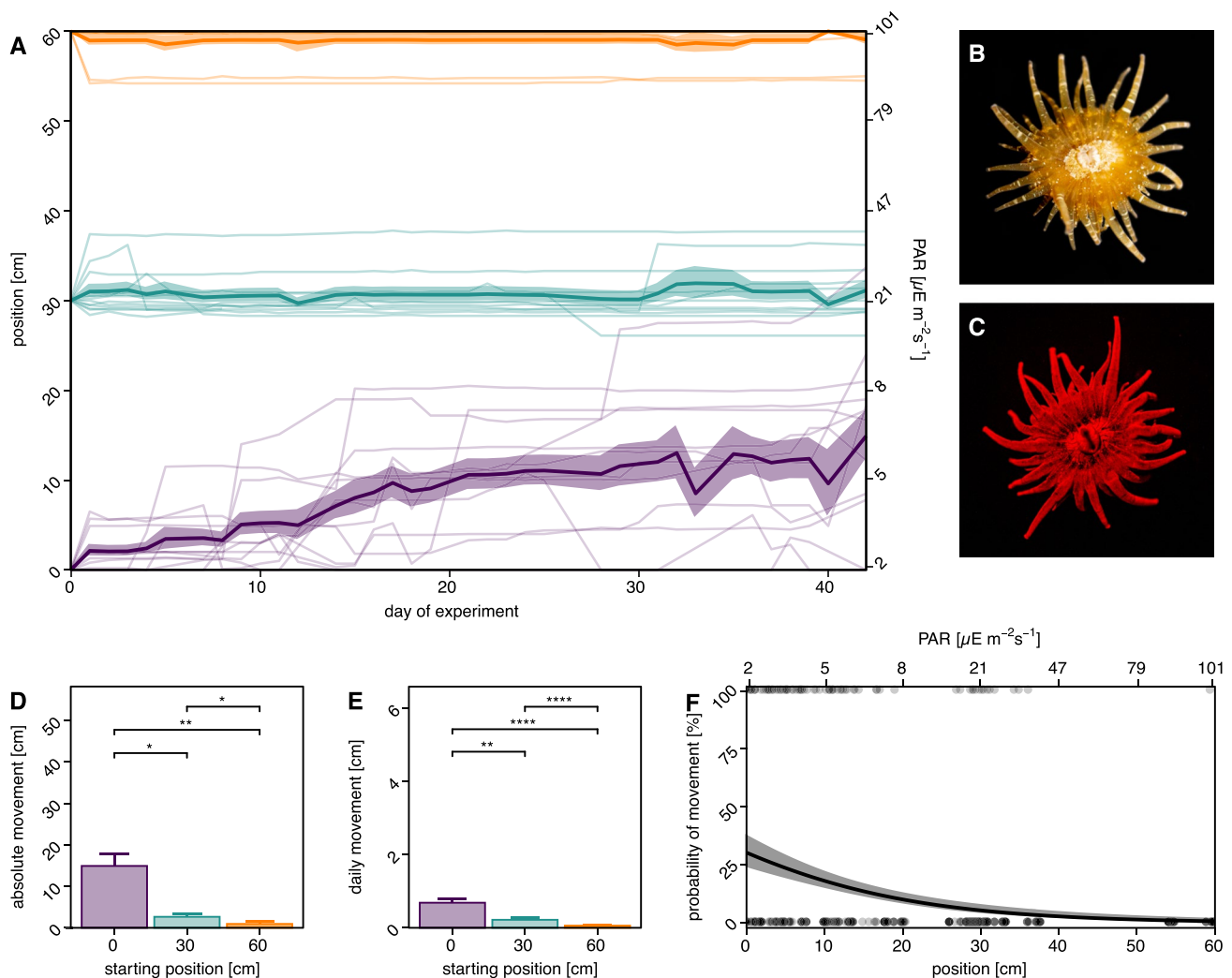


**Fig. 2** Movement of photosymbiotic Aiptasia along the light gradient. Three groups of animals were assessed based on their starting position corresponding to different light fields: purple—low light quantity, green—intermediate light quantity, yellow—high light quantity. **(A)** Movement along the gradient over the course of 42 days grouped by starting position. Thin lines represent movement of individuals, thick lines represent the daily group mean; the surrounding shaded areas represent the standard error of the mean. **(B)** Image of photosymbiotic Aiptasia. **(C)** Image of chlorophyll fluorescence by the endosymbiotic Symbiodiniaceae of photosymbiotic Aiptasia. **(D)**

Mean total distance travelled by animals after 42 days relative to the respective starting position. **(E)** Mean absolute daily movement over the course of 42 days by starting position. All error bars represent standard error, significance markers represent pairwise Wilcoxon–Mann–Whitney-test p-values (\*\*\* < 0.001, \*\* < 0.01, \* < 0.05). **(F)** Probability of daily movement along the light gradient. Points represent presence of movement (100%) or absence of movement (0%). The curve represents the modelled probability of movement at a given position, the surrounding shaded area represents the 95% confidence interval of the model

and  $\sim 101 \mu\text{E m}^{-2} \text{s}^{-1}$ ) showed a tendency towards the middle of the box during the experiment. The individual movements observed were greater than the individual movements of the photosymbiotic animals. The mean end positions of the animals starting at low, intermediate, and high light were  $33.6 \pm 6.8 \text{ cm}$  ( $\sim 29.1 \mu\text{E m}^{-2} \text{s}^{-1}$ ),  $18.4 \pm 4.9 \text{ cm}$  ( $\sim 7.0 \mu\text{E m}^{-2} \text{s}^{-1}$ ), and  $41.4 \pm 5.5 \text{ cm}$  ( $\sim 51.3 \mu\text{E m}^{-2} \text{s}^{-1}$ ), respectively.

The overall mean absolute distance was not significantly affected by the starting position (ANOVA,  $F = 3.14$ ,  $p\text{-value} = 0.057$ ) (Fig. 3D).

The mean absolute daily movement of aposymbiotic animals (Fig. 3E) differed significantly among the starting positions (Kruskal–Wallis test,  $\chi^2 = 11.97$ ,  $p\text{-value} = 0.003$ ). The difference in mean absolute daily movement was significant between animals starting at the intermediate position and animals starting at the bright end of the light gradient (pairwise Wilcoxon–Mann–Whitney test,  $p\text{-value} = 0.001$ ), while being insignificant between any two other starting positions.

The overall occurrence of movements  $\geq 0.5 \text{ cm d}^{-1}$  (46.5%) was significantly greater for aposymbiotic animals than for photosymbiotic animals (9.1%)

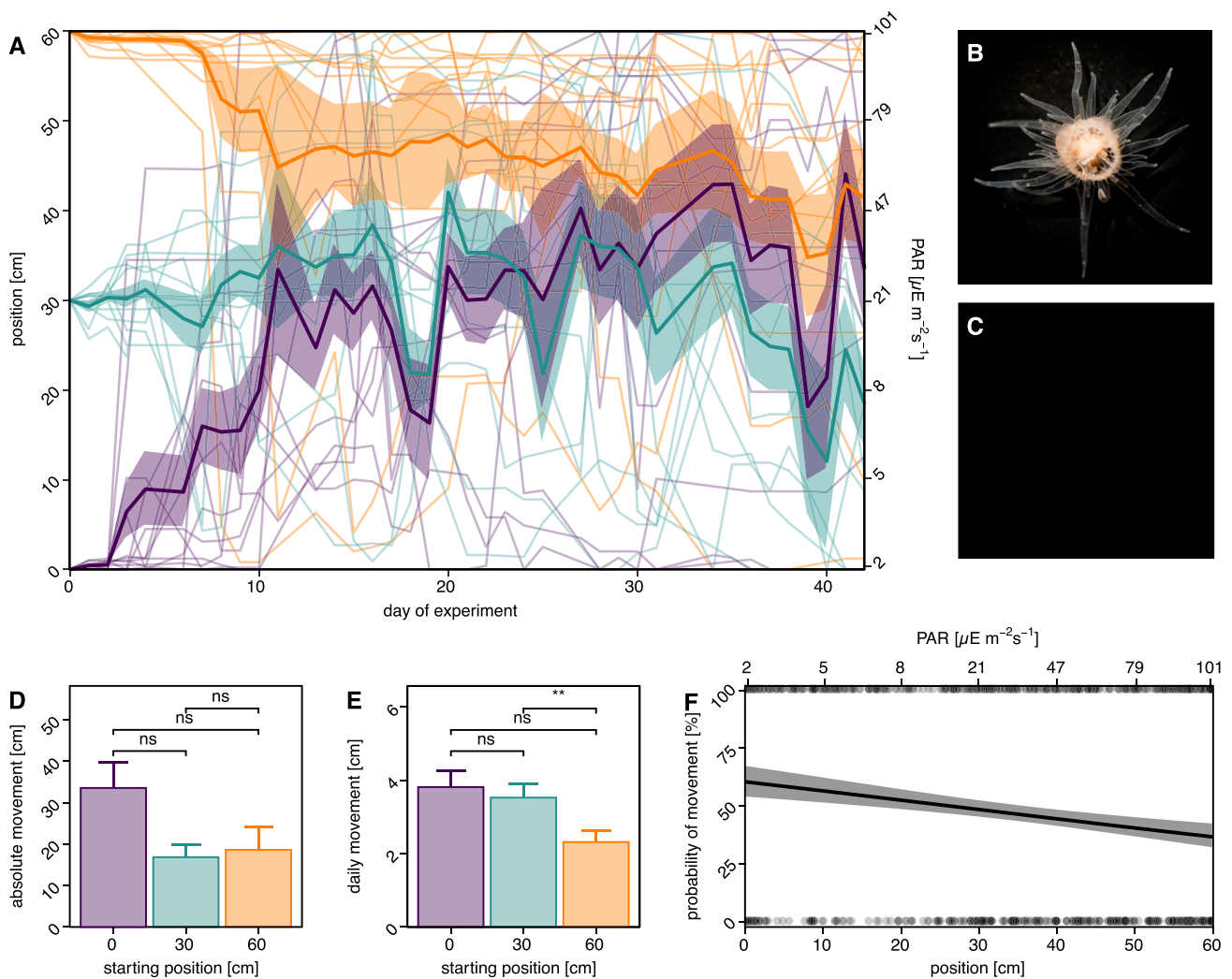


**Fig. 3** Movement of aposymbiotic Aiptasia along the light gradient. Three groups of animals were assessed based on their starting position corresponding to different light fields: purple—low light quantity, green—intermediate light quantity, yellow—high light quantity. **(A)** Movement along the light gradient over the course of 42 days grouped by starting position. Thin lines represent movement of individuals, thick lines represent the daily group mean; the surrounding shaded areas represent the standard error of the mean. **(B)** Image of aposymbiotic Aiptasia. **(C)** Image of chlorophyll fluorescence of aposymbiotic Aiptasia. Note that no fluorescence is visible due to the absence of endosymbiotic Symbiodiniaceae. **(D)** Mean total distance

( $\chi^2 = 321.71$ ,  $p$ -value  $< 0.001$ ). A lower incidence of locomotion was observed at increasing PAR levels (Fig. 3F). The probability of movement when plotted followed a linear distribution (McFadden  $R^2 = 0.018$ ;  $\chi^2 = 21.46$ ,  $p$ -value  $< 0.001$ ) with movement probability declining at greater PAR levels (from 60.5% at  $2 \mu\text{E m}^{-2} \text{s}^{-1}$  to 38.8% at  $101 \mu\text{E m}^{-2} \text{s}^{-1}$ ).

travelled by animals after 42 days relative to the respective starting position. **(E)** Mean absolute daily movement over the course of 42 days by starting position. All error bars represent standard error, significance markers represent in **(D)** Tukey-HSD  $p$ -values, and in **(E)** Wilcoxon-Mann-Whitney-test  $p$ -values ( $*** < 0.001$ ,  $** < 0.01$ ,  $* < 0.05$ ). **(F)** Probability of daily movement along the light gradient. Points represent presence of movement (100%) or absence of movement (0%). The curve represents the modelled probability of movement at a given position, the surrounding shaded area represents the 95% confidence interval of the model

### 3.2 Net photosynthesis along a light gradient

To assess whether the movement along the light gradient aligned with holobiont photophysiology, net photosynthesis rates along the gradient were determined (Fig. 4). Net photosynthetic rates of photosymbiotic Aiptasia in relation to light availability (PAR levels) followed a binomial distribution,

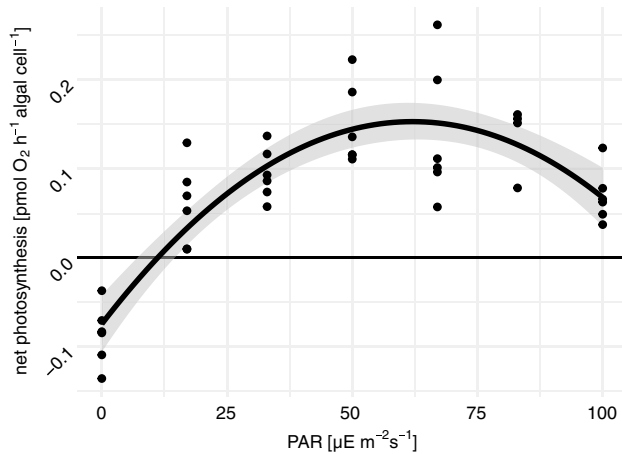


**Fig. 4** Net photosynthesis rates of photosymbiotic Aiptasia in relation to the available light quantity. Net photosynthesis rates are expressed as  $O_2$  flux normalized to microalgal symbiont densities in the measured anemones. Plotted points represent measurements of individual animals, the optimum curve represents the fitted model, and the surrounding shaded area represents the 95 % confidence interval of the model.

typical of an optimum curve,  $R^2 = 0.745$ ; overall F-test:  $F = 54.07$ ,  $p$ -value  $< 0.001$ ). Animals showed positive net photosynthesis rates (net  $O_2$  flux) at all investigated light levels ( $17$ – $100 \mu E m^{-2} s^{-1}$ ) except at absolute darkness ( $0 \mu E m^{-2} s^{-1}$ ). Based on the modeled distribution, the maximal net photosynthesis rate was at light levels of  $62 \mu E m^{-2} s^{-1}$  (likely in part reflecting acclimation to the culturing conditions), and the low-light compensation point ( $0 \text{ pmol } O_2 h^{-1} \text{ algal-cell}^{-1}$ ) was at light levels of  $11 \mu E m^{-2} s^{-1}$  (Fig. 4).

## 4 Discussion

Aiptasia exhibits a semi-sessile lifestyle, and its locomotive behavior is influenced by the presence of algal symbionts and its nutritional state (Foo et al. 2019; Bedgood et al. 2020). Here we demonstrate that photosymbiotic Aiptasia show increased locomotive behavior in low light compared to higher light quantities. Further, we observed that the probability of movement decreases exponentially with increasing light quantity in photosymbiotic Aiptasia, while this effect is less pronounced and non-exponential in aposymbiotic Aiptasia. This light-dependent behavior of photosymbiotic Aiptasia results in a net movement towards the light at low light quantities, i.e., phototaxis.

### 4.1 Light-dependent locomotion in Aiptasia

We observed that photosymbiotic Aiptasia starting at low light quantity in the light gradient exhibited greater absolute movement, whereas anemones starting in the high light

position exhibited considerably less absolute movement over the course of the experiment. Aposymbiotic Aiptasia on the other hand moved greater distances and the probability of movement was consistently greater along the entire light gradient. Notably, individual daily movements of both photo- and aposymbiotic Aiptasia did not appear to show consistent directionality along the light gradient.

Despite the lack of directionality of individual movements along the light gradient, we observed clear net locomotion towards increasing light quantity in photosymbiotic Aiptasia starting in the dark. Importantly, animals starting in the dark had initially one possible direction of movement. However, this also applied to animals starting in high light conditions, where no significant locomotion was recorded. Consequently, the observation of light dependent movement is unlikely to be confounded by the experimental design. Anemones exhibited greater movement probability (albeit non-directional) at low light, which decreased exponentially with increasing light quantity. By comparison, aposymbiotic Aiptasia exhibited a greater probability of movement at any given light intensity and a less pronounced effect of light on the net direction of movement. Importantly, we did not distinguish between modes of movement (i.e., crawling vs. detachment and floating). It is thus possible that differences in movement are the result of different detachment rates rather than active crawling in Aiptasia. The observed phototaxis in photosymbiotic Aiptasia appears to be the result of random locomotion in combination with the photonastic suppression of locomotion. Algal symbionts appear to play a central role in the observed locomotive behavior.

### 4.2 Nutritional state as a potential modulator of host locomotion

Our data suggest that photosynthesis may suppress locomotion in Aiptasia. At the end of the experiment, the mean position of animals starting in the dark approached the predicted compensation point of net photosynthesis for Aiptasia adapted to intermediate light conditions. While not all animals had moved to light levels sufficient for positive net photosynthesis, Aiptasia at light levels exceeding the predicted compensation point showed strongly reduced locomotion. Given sufficient time, it is thus plausible to assume that all animals would eventually move to light levels sufficient to support positive net photosynthesis. This suggests that net productivity in the symbiosis is an important driver of locomotion in (photosymbiotic) Aiptasia.

Indeed, a direct connection between photosynthesis products and locomotion/phototaxis has been observed in *A. elegantissima* where  $O_2$  supply has been demonstrated to suppress phototaxis in photosymbiotic animals (Fredericks 1976). In addition, it is also known that the hypoxic state in actinarian tissues can be avoided through symbiont

photosynthesis (Rands et al. 1992). Hence,  $O_2$  as a modulator of locomotion could explain not only the absence of locomotion in photosymbiotic animals at sufficient light quantity but also the more frequent occurrence of locomotion at low light quantities and in aposymbiotic animals. In this scenario, animals experience low  $O_2$  conditions because  $O_2$  consumption through respiration is greater than  $O_2$  production through photosynthesis. Hence, their probability of locomotive movement could be increased. Conversely, locomotion will be suppressed if sufficient  $O_2$  is available, i.e., at light levels higher than the compensation point of net photosynthesis. However, it has been demonstrated that heterotrophic feeding suppresses locomotion in *Aiptasia* with high and low symbiont densities, respectively (Bedgood et al. 2020). This phenomenon cannot be explained by  $O_2$  as the sole modulator of locomotion. In fact, increased availability of heterotrophic nutrition would result in increased respiration, thereby reducing  $O_2$  levels. At least in *Aiptasia* evidence suggests that the nutritional state (i.e., starvation, lack of substrate for energy metabolism) modulates locomotion. *Aiptasia* can avoid starvation through the uptake of energy-rich organic nutrients. This can happen either by heterotrophic feeding or by phototrophic assimilation of photosynthates in the algal symbiont and their subsequent translocation to the host (Falkowski et al. 1984). At sufficient light quantity, the algal symbionts will produce and translocate enough photosynthate to avoid starvation of the host. If starvation can be avoided, locomotion will be suppressed as there is no need to optimize nutrient translocation through locomotion; the rule here may be “to *Aiptasia*, good enough means perfect”. Our results also suggest that below the photosynthetic compensation point the suppression of locomotion is correlated with light quantity. We conclude that sufficient symbiotic nutrient translocation covering the metabolic energy demands of the host may suppress locomotive activity in *Aiptasia*.

The hypothesis of nutrient-controlled phototaxis suggests that phototaxis can emerge as the result of starvation-induced and nutrient-suppressed locomotion in photosymbiotic animal systems. Increased locomotive activity under starvation conditions is a common phenomenon observed in many biological systems (Van Haastert and Bosgraaf 2009; Yang et al. 2015). In (photo)symbiotic systems governed by nutrient cycling, phototaxis can readily emerge from otherwise non-directional locomotive behavior, even if the locomotive organism itself may not be specifically adapted to perform phototaxis.

### 4.3 Implications for the study of cnidarian-algal symbioses

Although our results suggest the presence of a photosynthesis-derived modulator of phototaxis, we cannot currently

deduce the nature of such a modulator in *Aiptasia* because we did not investigate the effect of  $O_2$  or heterotrophic feeding on locomotion. The nature of the effect of photosynthate translocation on locomotion or phototaxis should be investigated further through experiments featuring for instance inhibition of photosynthesis, photosynthate substitution (e.g., feeding with glucose, glycerol, *Artemia*, etc.), and  $O_2$  manipulation. Such experiments will help to contextualize the findings regarding the role of food availability and  $O_2$  in the phototactic behavior of *A. elegantissima* (Pearse 1974; Fredericks 1976) and *Aiptasia* (Bedgood et al. 2020 and this study). In our study, we observed only a narrow light gradient and it is possible that *Aiptasia* exhibit negative phototaxis above a certain light quantity. According to our nutrient-controlled phototaxis hypothesis, this could also be the result of reduced production and translocation of photosynthesis products due to photodamage causing an energy deficit. Negative phototaxis has been previously observed in *A. elegantissima* from shaded habitats (Pearse 1974). Additionally, we exposed animals to permanent light conditions in the present study. However, natural diurnal light variability imposes circadian oscillations in photophysiology of Symbiodiniaceae and imposes a rhythmicity of nutrient availability and oxidative stress on the symbiosis (Hoegh-Guldberg and Jones 1999; Hill and Ralph 2005). Therefore, future studies looking into the phototactic behavior of *Aiptasia* should simulate natural light conditions, i.e., include greater light quantities sufficient to impose oxidative stress and consider the circadian aspects of photosynthesis. Especially at higher light quantities, photoinhibition and oxidative stress may have a role in anemone movement.

*Aiptasia* phototaxis may also be influenced by host photoreception. We cannot currently exclude a host effect on *Aiptasia* phototaxis (see the observed linear decrease of movement probability with increasing light quantity in aposymbiotic animals), although previous studies suggest that phototaxis only occurs in photosymbiotic Actiniaria (Pearse 1974; Foo et al. 2019). In other Cnidaria, phototaxis readily occurs in aposymbiotic or algal symbiont-depleted animals, e.g., in Fungiidae and *Hydra* (Wilson 1891; Yamashiro and Nishira 1995). This is probably due to the ability of cnidarian polyps to perceive light by extraocular photoreception (i.e., perception by diffusely distributed photoreceptive cells, not organized in sensory organs) (as reviewed by Martin (2002)) with an array of photoreceptors, of which opsins have received the greatest attention (Plachetzki et al. 2007; Vocking et al. 2017). Interestingly, the expression profiles of opsins in *Aiptasia* differ between photosymbiotic and aposymbiotic animals (Gornik et al. 2021), indicating an algal symbiont-induced change in the photosensory makeup of the host, which in turn might affect locomotive behavior in the way we observed. Some cnidarian light responses are known to be photoreceptor-dependent, for example cnidocyte

discharge upon shading and tentacle retraction upon illumination with blue light (Gorbunov and Falkowski 2002; Plachetzki et al. 2012). Therefore, the role of actinarian photoreceptors in phototaxis deserves further assessment.

Finally, our results also hold implications for scleractinian reef corals. Scleractinian coral larvae exhibit phototaxis for settlement, even when still aposymbiotic (e.g., in *Acropora tenuis* and *A. millepora*) (Mundy and Babcock 1998; Strader et al. 2015). It is conceivable that in corals with photosymbiotic larvae, settlement is directly modulated by photosynthesis products of the algal symbiont (see also Mies et al. 2017). Under too little light, insufficient photosynthate translocation and therefore starvation may stimulate the search for a more suitable habitat, whereas in habitats with more suitable light conditions, translocated nutrients may suppress further locomotion, i.e., search behavior. Another larval phototactic behavior possibly influenced by symbiotic nutrient translocation is dispersal, as observed in the coral *Pocillopora verrucosa*. Photosymbiotic larvae have been shown to phototact towards the sea surface to increase their dispersal distance, while energy supply during dispersal is provided by the algal symbionts (Mulla et al. 2021). Hence, algal symbionts likely have a major effect on the behavior of the host and as such the behavior and ecology of the holobiont as a whole. In this light, the development of starvation-induced phototaxis could offer a powerful model to study the metabolic interactions underlying symbiont-controlled behavior of the host.

#### 4.4 Conclusions

We found that light quantity influences locomotion in photosymbiotic *Aiptasia* as the probability of movement declines exponentially with increasing light quantity. In contrast, this effect of light availability on movement is less pronounced and non-exponential in aposymbiotic *Aiptasia*. These effects may be explained by the modulation of the locomotive behavior of the host by photosynthate translocation from its algal symbionts. Although our findings are based on a specific host-symbiont combination, our proposed model of nutrition-dependent locomotion may also serve to explain phototactic behavior in other photosymbioses. We conclude that complex behaviors such as phototaxis may arise as an indirect consequence of symbiotic nutrient cycling. This highlights that even behavioral traits need to be interpreted under consideration of the underlying metabolic interactions within complex holobionts.

**Acknowledgements** The authors would like to thank the Scientific Engineering Services (Wissenschaftliche Werkstätten) at the University of Konstanz for their support with the design and construction of the experimental boxes. Further, the authors thank D. Jovicic for the generation of aposymbiotic *Aiptasia* and acknowledge assistance by K. Bär-Hage, P. Merkel, and M. Schmid with *Aiptasia* husbandry.

**Author contribution** NFS, NR, CP, and CRV conceived and designed the experiment. NFS conducted the experiment and analyzed the data. All authors contributed to the writing and revision of the manuscript.

**Funding** Open Access funding enabled and organized by Projekt DEAL. NR, CP and CRV would like to acknowledge AFF funding (Project MetaFit; grant number 15902919 FP 029/19). NR and AM are supported by the Swiss National Science Foundation, grant 200021\_179092.

**Data availability** All experimental data associated with this experiment has been deposited at Zenodo.org and are freely available at <https://doi.org/10.5281/zenodo.5036902> (Strumpen et al. 2021).

#### Declarations

**Competing interests** The authors declare no conflicts of interest.

**Open Access** This article is licensed under a Creative Commons Attribution 4.0 International License, which permits use, sharing, adaptation, distribution and reproduction in any medium or format, as long as you give appropriate credit to the original author(s) and the source, provide a link to the Creative Commons licence, and indicate if changes were made. The images or other third party material in this article are included in the article's Creative Commons licence, unless indicated otherwise in a credit line to the material. If material is not included in the article's Creative Commons licence and your intended use is not permitted by statutory regulation or exceeds the permitted use, you will need to obtain permission directly from the copyright holder. To view a copy of this licence, visit <http://creativecommons.org/licenses/by/4.0/>.

#### References

- Anthony KR, Fabricius KE (2000) Shifting roles of heterotrophy and autotrophy in coral energetics under varying turbidity. *J Exp Mar Biol Ecol* 252:221–253. [https://doi.org/10.1016/S0022-0981\(00\)00237-9](https://doi.org/10.1016/S0022-0981(00)00237-9)
- Anthony KR, Ridd PV, Orpin AR, Larcombe P, Lough J (2004) Temporal variation of light availability in coastal benthic habitats: Effects of clouds, turbidity, and tides. *Limnol Oceanogr* 49:2201–2211. <https://doi.org/10.4319/lo.2004.49.6.2201>
- Baker PA, Weber JN (1975) Coral growth rate: Variation with depth. *Earth Planet Sci Lett* 27:57–61. [https://doi.org/10.1016/0012-821X\(75\)90160-0](https://doi.org/10.1016/0012-821X(75)90160-0)
- Baumgarten S, Simakov O, Esherick LY, Liew YJ, Lehnert EM, Mitchell CT, Li Y, Hambleton EA, Guse A, Oates ME, Gough J, Weis VM, Aranda M, Pringle JR, Voolstra CR (2015) The genome of *Aiptasia*, a sea anemone model for coral symbiosis. *Proc Natl Acad Sci* 112:11893–11898. <https://doi.org/10.1073/pnas.1513318112>
- Bedgood SA, Bracken MES, Ryan WH, Levell ST, Wulff J (2020) Nutritional drivers of adult locomotion and asexual reproduction in a symbiont-hosting sea anemone *Exaiptasia diaphana*. *Mar Biol* 167:39. <https://doi.org/10.1007/s00227-020-3649-3>
- Bieri T, Onishi M, Xiang T, Grossman AR, Pringle JR (2016) Relative contributions of various cellular mechanisms to loss of Algae during cnidarian bleaching. *PLoS ONE* 11:e0152693. <https://doi.org/10.1371/journal.pone.0152693>
- Cook C, D'Elia C, Muller-Parker G (1988) Host feeding and nutrient sufficiency for zooxanthellae in the sea anemone *Aiptasia*

- pallida*. Mar Biol 98:253–262. <https://doi.org/10.1007/BF00391203>
- Cooper TF, Ulstrup KE, Dandan SS, Heyward AJ, Kühl M, Muirhead A, O’Leary RA, Ziersen BE, Van Oppen MJ (2011) Niche specialization of reef-building corals in the mesophotic zone: metabolic trade-offs between divergent *Symbiodinium* types. Proc R Soc B: Biol Sci 278:1840–1850. <https://doi.org/10.1098/rspb.2010.2321>
- Dungan AM, Hartman LM, Tortorelli G, Belderok R, Lamb AM, Pisan L, McFadden GI, Blackall LL, van Oppen MJ (2020) *Exaiptasia diaphana* from the great barrier reef: a valuable resource for coral symbiosis research. Symbiosis 1–12. <https://doi.org/10.1007/s13199-020-00665-0>
- Eberhard S, Finazzi G, Wollman FA (2008) The dynamics of photosynthesis. Annu Rev Genet 42:463–515. <https://doi.org/10.1146/annurev.genet.42.110807.091452>
- Falkowski PG, Dubinsky Z, Muscatine L, Porter JW (1984) Light and the bioenergetics of a symbiotic coral. Bioscience 34:705–709. <https://doi.org/10.2307/1309663>
- Foo SA, Liddell L, Grossman A, Caldeira K (2019) Photo-movement in the sea anemone *Aiptasia* influenced by light quality and symbiotic association. Coral Reefs 39:47–54. <https://doi.org/10.1007/s00338-019-01866-w>
- Frade P, Englebert N, Faria J, Visser P, Bak R (2008) Distribution and photobiology of *Symbiodinium* types in different light environments for three colour morphs of the coral *Madracis pharensis*: is there more to it than total irradiance? Coral Reefs 27:913–925. <https://doi.org/10.1007/s00338-008-0406-3>
- Fredericks CA (1976) Oxygen as a limiting factor in phototaxis and in intracolonial spacing of the sea anemone *Anthopleura elegantissima*. Mar Biol 38:25–28. <https://doi.org/10.1007/BF00391482>
- Furla P, Galgani I, Durand I, Allemand D (2000) Sources and mechanisms of inorganic carbon transport for coral calcification and photosynthesis. J Exp Biol 203:3445–3457. <https://doi.org/10.1242/jeb.203.22.3445>
- Gorbanov MY, Falkowski PG (2002) Photoreceptors in the cnidarian hosts allow symbiotic corals to sense blue moonlight. Limnol Oceanogr 47:309–315. <https://doi.org/10.4319/lo.2002.47.1.0309>
- Gornik SG, Berghem BG, Morel B, Stamatakis A, Foulkes NS, Guse A (2021) Photoreceptor diversification accompanies the evolution of Anthozoa. Mol Biol Evol 38:1744–1760. <https://doi.org/10.1093/molbev/msaa304>
- Grigg RW (2005) Depth limit for reef building corals in the Au’au Channel, S.E. Hawaii Coral Reefs 25:77–84. <https://doi.org/10.1007/s00338-005-0073-6>
- Highsmith RC (1982) Reproduction by fragmentation in corals. Mar Ecol Progress Ser Oldendorf 7:207–226
- Hill R, Ralph PJ (2005) Diel and seasonal changes in fluorescence rise kinetics of three scleractinian corals. Funct Plant Biol 32:549–559. <https://doi.org/10.1071/FP05017>
- Hoegh-Guldberg O, Jones RJ (1999) Photoinhibition and photoprotection in symbiotic dinoflagellates from reef-building corals. Mar Ecol Prog Ser 183:73–86. <https://doi.org/10.3354/meps183073>
- Iglesias-Prieto R, Beltran VH, LaJeunesse TC, Reyes-Bonilla H, Thome PE (2004) Different algal symbionts explain the vertical distribution of dominant reef corals in the eastern Pacific. Proc R Soc Lond Ser B: Biol Sci 271:1757–1763. <https://doi.org/10.1098/rspb.2004.2757>
- Iwatsuki K, Naitoh Y (1981) The role of Symbiotic Chlorella in Photoresponses of *Paramecium bursaria*. Proc Jpn Acad Ser B 57:318–323. <https://doi.org/10.2183/pjab.57.318>
- Jekely G (2009) Evolution of phototaxis. Trans R Soc B Biol Sci 364:2795–2808. <https://doi.org/10.1098/rstb.2009.0072>
- Kahng SE, Hochberg EJ, Apprill A, Wagner D, Luck DG, Perez D, Bidigare RR (2012) Efficient light harvesting in deep-water zooxanthellate corals. Mar Ecol Prog Ser 455:65–77. <https://doi.org/10.3354/meps09657>
- Kaniewska P, Magnusson SH, Anthony KR, Reef R, Kühl M, Hoegh-Guldberg O (2011) Importance of macro- versus microstructure in modulating light levels inside coral colonies. J Phycol 47:846–860. <https://doi.org/10.1111/j.1529-8817.2011.01021.x>
- Kleypas JA, McManus JW, Menez LA (1999) Environmental limits to coral reef development: Where do we draw the line? Am Zool 39:146–159. <https://doi.org/10.1093/icb/39.1.146>
- Kopp C, Domart-Coulon I, Escrig S, Humbel BM, Hignette M, Meibom A (2015) Subcellular investigation of photosynthesis-driven carbon assimilation in the symbiotic reef coral *Pocillopora damicornis*. Mbio 6:e02299–e2214. <https://doi.org/10.1128/mBio.02299-14>
- LaJeunesse TC, Parkinson JE, Gabrielson PW, Jeong HJ, Reimer JD, Voolstra CR, Santos SR (2018) Systematic Revision of Symbiodiniaceae Highlights the Antiquity and Diversity of Coral Endosymbionts. Curr Biol 28:2570–2580.e6. <https://doi.org/10.1016/j.cub.2018.07.008>
- Martin VJ (2002) Photoreceptors of cnidarians. Can J Zool 80:1703–1722. <https://doi.org/10.1139/z02-136>
- Mies M, Sumida PYG, Rädicker N, Voolstra CR (2017) Marine invertebrate larvae associated with Symbiodinium: A mutualism from the start? Front Ecol Evol 5:56. <https://doi.org/10.3389/fevo.2017.00056>
- Miyamoto A, Sakai A, Nakano R, Yusa Y (2015) Phototaxis of sacoglossan sea slugs with different photosynthetic abilities: a test of the ‘crawling leaves’ hypothesis. Mar Biol 162:1343–1349. <https://doi.org/10.1007/s00227-015-2673-1>
- Muir PR, Wallace CC, Done T, Aguirre JD (2015) Coral reefs. Limited scope for latitudinal extension of reef corals. Science 348:1135–1138. <https://doi.org/10.1126/science.1259911>
- Mulla AJ, Lin C-H, Takahashi S, Nozawa Y (2021) Photo-movement of coral larvae influences vertical positioning in the ocean. Coral Reefs 1–10. <https://doi.org/10.1007/s00338-021-02141-7>
- Mundy C, Babcock R (1998) Role of light intensity and spectral quality in coral settlement: Implications for depth-dependent settlement? J Exp Mar Biol Ecol 223:235–255. [https://doi.org/10.1016/S0022-0981\(97\)00167-6](https://doi.org/10.1016/S0022-0981(97)00167-6)
- Muscatine L, Porter JW (1977) Reef corals: Mutualistic symbioses adapted to nutrient-poor environments. Bioscience 27:454–460. <https://doi.org/10.2307/1297526>
- Muscatine L, Porter JW, Kaplan IR (1989) Resource partitioning by reef corals as determined from stable isotope composition. Mar Biol 100:185–193. <https://doi.org/10.1007/bf00391957>
- Olito C, White CR, Marshall DJ, Barneche DR (2017) Estimating monotonic rates from biological data using local linear regression. J Exp Biol 220:759–764. <https://doi.org/10.1242/jeb.148775>
- Papina M, Meziane T, van Woesik R (2003) Symbiotic zooxanthellae provide the host-coral *Montipora digitata* with polyunsaturated fatty acids. Comp Biochem Physiol B Biochem Mol Biol 135:533–537. [https://doi.org/10.1016/s1096-4959\(03\)00118-0](https://doi.org/10.1016/s1096-4959(03)00118-0)
- Pearse VB (1974) Modification of sea anemone behavior by symbiotic zooxanthellae: phototaxis. Biol Bull 147:630–640. <https://doi.org/10.2307/1540746>
- Plachetzki DC, Degnan BM, Oakley TH (2007) The origins of novel protein interactions during animal opsin evolution. PLoS ONE 2:e1054. <https://doi.org/10.1371/journal.pone.0001054>
- Plachetzki DC, Fong CR, Oakley TH (2012) Cnidocyte discharge is regulated by light and opsin-mediated phototransduction. BMC Biol 10:1–10. <https://doi.org/10.1186/1741-7007-10-17>
- Pringle Lab (2018) Cold-shock protocol to bleach *Aiptasia* v1 (protocols.io.qx8dxrw). <https://doi.org/10.17504/protocols.io.qx8dxrw>
- R Core Team (2020) R: A language and environment for statistical computing. R Foundation for Statistical Computing, Vienna, Austria

- Rädecker N, Pogoreutz C, Voolstra CR, Wiedenmann J, Wild C (2015) Nitrogen cycling in corals: the key to understanding holobiont functioning? *Trends Microbiol* 23:490–497. <https://doi.org/10.1016/j.tim.2015.03.008>
- Rädecker N, Pogoreutz C, Gegner HM, Cárdenas A, Roth F, Bougoure J, Guagliardo P, Wild C, Pernice M, Raina J-B, Meibom A, Voolstra CR (2021) Heat stress destabilizes symbiotic nutrient cycling in corals. *Proc Natl Acad Sci* 118:e2022653118. <https://doi.org/10.1073/pnas.2022653118>
- Rands ML, Douglas AE, Loughman BC, Ratcliffe RG (1992) Avoidance of Hypoxia in a cnidarian symbiosis by algal photosynthetic oxygen. *Biol Bull* 182:159–162. <https://doi.org/10.2307/1542191>
- Riemann-Zürneck K (1998) How sessile are sea anemones? A review of free-living forms in the Actiniaria Cnidaria: Anthozoa. *Mar Ecol* 19:247–261. <https://doi.org/10.1111/j.1439-0485.1998.tb00466.x>
- Rowan R, Knowlton N (1995) Intraspecific diversity and ecological zonation in coral-algal symbiosis. *Proc Natl Acad Sci* 92:2850–2853. <https://doi.org/10.1073/pnas.92.7.2850>
- Salih A, Larkum A, Cox G, Kuhl M, Hoegh-Guldberg O (2000) Fluorescent pigments in corals are photoprotective. *Nature* 408:850–853. <https://doi.org/10.1038/35048564>
- Seródio J, Silva R, Ezequiel J, Calado R (2011) Photobiology of the symbiotic acoel flatworm *Symsagittifera roscoffensis*: algal symbiont photoacclimation and host photobehaviour. *Marine Biological Association of the United Kingdom. J Mar Biol Assoc U K* 91:163. <https://doi.org/10.1017/S0025315410001001>
- Sheppard C, Davy S, Pilling G, Graham N (2017) *The biology of coral reefs*. Oxford University Press
- Smith EG, D'angelo C, Sharon Y, Tchernov D, Wiedenmann J (2017) Acclimatization of symbiotic corals to mesophotic light environments through wavelength transformation by fluorescent protein pigments. *Proc R Soc B: Biol Sci* 284:20170320. <https://doi.org/10.1098/rspb.2017.0320>
- Strader ME, Davies SW, Matz MV (2015) Differential responses of coral larvae to the colour of ambient light guide them to suitable settlement microhabitat. *R Soc Open Sci* 2:150358. <https://doi.org/10.1098/rsos.150358>
- Strumpen NF, Rädecker N, Pogoreutz C, Voolstra CR (2021) Light quantity controls locomotion in photosymbiotic *Aiptasia*. *Zenodo*. <https://doi.org/10.5281/zenodo.5036902>
- Sunagawa S, Wilson EC, Thaler M, Smith ML, Caruso C, Pringle JR, Weis VM, Medina M, Schwarz JA (2009) Generation and analysis of transcriptomic resources for a model system on the rise: the sea anemone *Aiptasia pallida* and its dinoflagellate endosymbiont. *BMC Genomics* 10:258. <https://doi.org/10.1186/1471-2164-10-258>
- Titlyanov E, Titlyanova T, Yamazato K, van Woesik R (2001) Photoacclimation dynamics of the coral *Stylophora pistillata* to low and extremely low light. *J Exp Mar Biol Ecol* 263:211–225. [https://doi.org/10.1016/S0022-0981\(01\)00309-4](https://doi.org/10.1016/S0022-0981(01)00309-4)
- Van Haastert PJ, Bosgraaf L (2009) Food Searching Strategy of Amoeboid cells by Starvation Induced Run Length Extension. *PLoS ONE* 4:e6814. <https://doi.org/10.1371/journal.pone.0006814>
- Vocking O, Kourtesis I, Tumu SC, Hausen H (2017) Co-expression of xenopsin and rhabdomic opsin in photoreceptors bearing microvilli and cilia. *Elife* 6:e23435. <https://doi.org/10.7554/eLife.23435>
- Wall CB, Kaluhiokalani M, Popp BN, Donahue MJ, Gates RD (2020) Divergent symbiont communities determine the physiology and nutrition of a reef coral across a light-availability gradient. *ISME J* 14:945–958. <https://doi.org/10.1038/s41396-019-0570-1>
- Weis VM, Davy SK, Hoegh-Guldberg O, Rodriguez-Lanetty M, Pringle JR (2008) Cell biology in model systems as the key to understanding corals. *Trends Ecol Evol* 23:369–376
- Wilson EB (1891) The heliotropism of *Hydra*. *Am Nat* 25:413–433
- Yamashiro H, Nishira M (1995) Phototaxis in Fungiidae corals (Scleractinia). *Mar Biol* 124:461–465. <https://doi.org/10.1007/BF00363920>
- Yang Z, Yu Y, Zhang V, Tian Y, Qi W, Wang L (2015) Octopamine mediates starvation-induced hyperactivity in adult *Drosophila*. *Proc Natl Acad Sci* 112:5219–5224. <https://doi.org/10.1073/pnas.1417838112>
- Ziegler M, Roder CM, Büchel C, Voolstra CR (2014) Limits to physiological plasticity of the coral *Pocillopora verrucosa* from the central Red Sea. *Coral Reefs* 33:1115–1129. <https://doi.org/10.1007/s00338-014-1192-8>
- Ziegler M, Roder C, Büchel C, Voolstra CR (2015a) Niche acclimatization in Red Sea corals is dependent on flexibility of host-symbiont association. *Mar Ecol Prog Ser* 533:149–161. <https://doi.org/10.3354/meps.11365>
- Ziegler M, Roder CM, Büchel C, Voolstra CR (2015b) Mesophotic coral depth acclimatization is a function of host-specific symbiont physiology. *Front Mar Sci* 2:4. <https://doi.org/10.3389/fmars.2015.00004>

**Publisher's note** Springer Nature remains neutral with regard to jurisdictional claims in published maps and institutional affiliations.